Analysis of Optical Single-Event Transients in Integrated Silicon Photonics Mach-Zehnder Modulators for Space-based Optical Communications

Mozhgan Hosseinzadeh, Jeffrey W. Teng, Brett L. Ringel, Delgermaa Nergui, Adrian Ildefonso, Ani Khachatrian, Dale McMorrow, and John D. Cressler

Student Paper

Abstract: Integrated SiPh MZMs are exposed to pulsed-laser-induced TPA, and the sensitivity to single-event transients is measured. A numerical model to predict the SET effects on SiPh MZM is developed, as well as a simulation path to validate the model.

Session Preference: Photonic Devices and Integrated Circuits

Presentation Preference: Oral

Acknowledgement
This work was supported in part by a grant from the United States Government, and the National Science Foundation, under the EPICA IUCRC at Georgia Tech. Device samples were obtained through GlobalFoundries multi-project wafer runs. We are grateful to R. Augur, N. Cahoun, A. Darbar, D. Eades, A. Joseph, and the GlobalFoundries SiGe team for device fabrication.

Corresponding Author:
Mozhgan Hosseinzadeh
School of Electrical and Computer Engineering, Georgia Institute of Technology,
777 Atlantic Drive NW, Atlanta, GA 30332-0250 USA
USA Phone: 470-815-4222
Email: mhosseinzadeh3@gatech.edu

Contributing Authors:
Jeffrey W. Teng, Brett L. Ringel, Delgermaa Nergui
John D. Cressler (cressler@ece.gatech.edu)
School of Electrical and Computer Engineering, Georgia Institute of Technology, Atlanta, GA 30332 USA

Adrian Ildefonso, Ani Khachatrian, Dale McMorrow
United States Naval Research Laboratory, Code 6816, Washington, DC 20375 USA

I. Introduction

Optical communications have proven to provide orders-of-magnitude higher data rates than conventional radio-frequency (RF) systems, making them suitable for next-generation deep-space missions. Current RF techniques are reaching their bandwidth limits due to limitations on transmitted power and removal of generated heat as the communication distance increases. The promised bandwidth of optical communications is much more since the operating carrier frequency of the signal is dramatically increased [1].

NASA's Deep Space Optical Communications (DSOC) program is currently investigating optical communications for Earth-Moon systems. The DSOC laser transceiver, featuring a near-infrared optical system, will be integrated with the Psyche spacecraft as it travels to a metal asteroid located between Mars and Jupiter [2].

For space-based systems, improvements in size, weight, power consumption, and cost (SWAP-C) are critical, which encourages the use of integrated circuits. Silicon Photonics (SiPh) technologies, which monolithically combine classical photonics and high-speed electronics, provide complex optical functionality in a small footprint and with excellent manufacturability, while providing compatibility with CMOS and SiGe electronic integrated circuits [3], [4].

As a key reliability concern, space systems must demonstrate immunity to the various effects of space radiation on electronic and photonic components [5]. Given the relative immaturity of the field, more knowledge of radiation effects in silicon photonic components is needed to ensure electronic-photonic integrated circuits (ePICs) are viable, robust substitutes for their RF counterparts.

Optical modulators are key components in optical links, where light is modulated with a stream of data. The silicon Mach-Zehnder modulator (MZM) is a popular type of SiPh modulator that has shown substantial total ionizing dose (TID) hardness, up to multi-Mrad(SiO_2) levels [6]. There is, however, only limited literature on single-event effects (SEEs) in SiPh modulators, as well as other photonic integrated circuit (PIC) components [7]–[9].

The present paper investigates for the first time the effects of single-event transients (SETs) on a standalone Si MZM. An additional aim is to provide a model for the numerical calculation of such SET events, as well as a simulation path to validate the model.

II. Experimental Setup

Si MZM can be described as two parallel pin phase shifters as the two branches of an interferometer. Applying voltage to each branch alters the optical length of that arm. By varying the voltage, the amount of constructive interference at the output of the MZM changes. The DC voltage to apply to a branch of the MZM to have a phase change of π is called V_π. The relationship between the applied Voltage and the output power of the MZM can be represented by a Mach-Zehnder transfer function [10].

Devices were fabricated on the GlobalFoundries 45SPCLO silicon photonics technology platform. Optical devices on this platform feature 160-nm thickness and support optical wavelengths in O-band (1310-nm light) [11]. 45SPCLO platform offers MZMs with roughly 35 GHz electrical bandwidth. Light is coupled to the integrated device via O-band grating couplers. Optical fiber array packaging enabled *in-situ* measurement capability at beam. A schematic cross-section of the MZM's arm is shown in Fig. 1

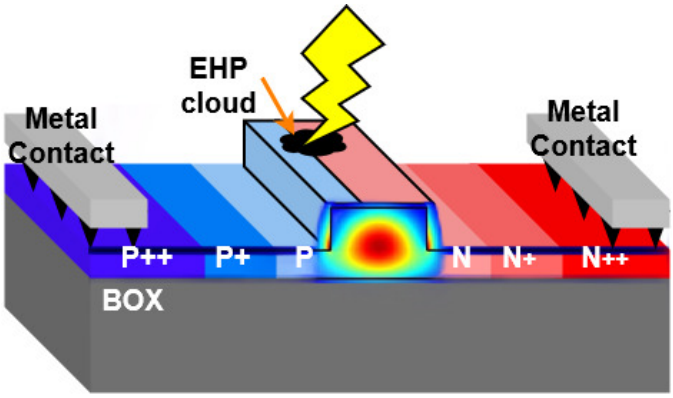

Fig. 1. Schematic cross-section of the tested MZM. Laser-induced electron-hole pairs (EHP) are shown. As seen in the figure, the optical mode propagating through the phase shifter interacts with a dense SET-generated EHP cloud. BOX refers to the buried-oxide layer under the Si layer.

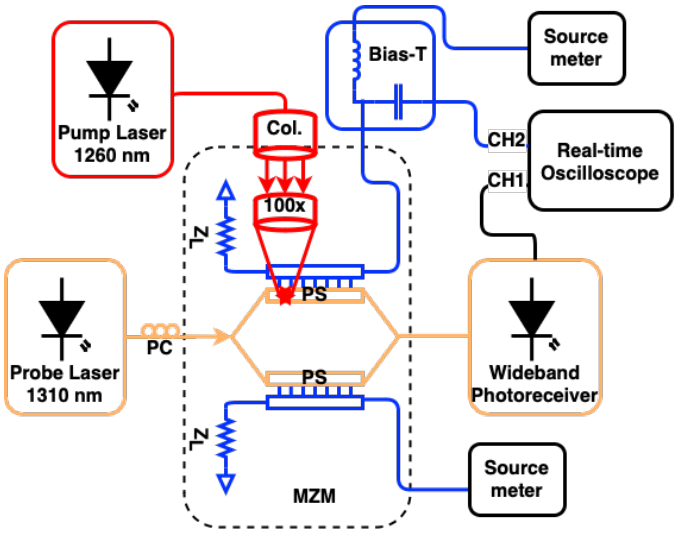

Fig. 2. A schematic diagram summarizing the experiment setup to capture OSETs in Si MZM.

The experimental setup is summarized in Fig. 2. The MZM structure comprises two parallel phase shifters, labeled PS in Fig. 2, each with a length of 2 mm, featuring a $V_\pi L$ figure-of-merit of 1.94 V-cm. Each phase shifter is biased separately with Keithley 2400 sourcemeters, and RF transients were collected using bias tees. Transient output signals were measured using a Tektronix MSO72004C mixed-signal oscilloscope with an analog bandwidth of 20 GHz and a sample rate of 100 GS/s.

Incoming continuous-wave (CW) probe laser with a fixed 1310-nm wavelength and 36 mW optical power couples through a packaged fiber array to the SiPh chip. Phase-shifted light from each arm is recombined, and via a fiber array, output light gets detected with the New Focus DC-12 GHz IR photoreceiver.

The experiment was conducted at the U.S. Naval Research Laboratory using 1260-nm laser pulses. The charge was deposited with two-photon absorption (TPA) process through the

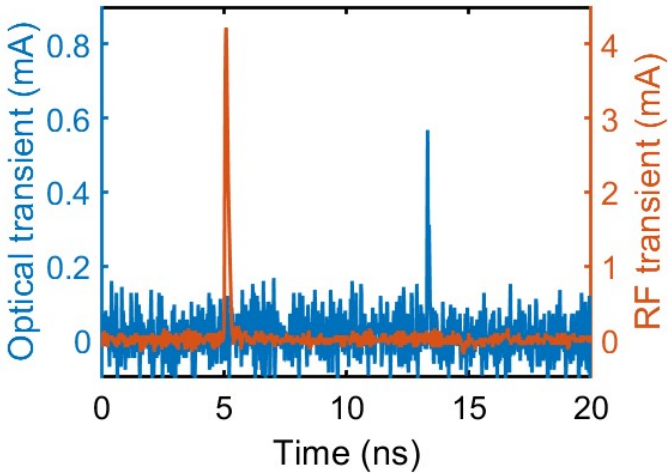

Fig. 3. Optical and RF transients of the tested MZM. Optical SETs appear at the detected output power of the device. Blue ■ = Optical transient. RF transients are measured at the metal contact of the excited phase shifter. Orange ■ = RF transient.

backside of the silicon die. The laser pulses were generated by an optical parametric amplifier using a Clark-MXR CPA2110 Ti: Sapphire system. A nominal laser pulse energy (PE) of 22 nJ was used for all tests. Pump laser pulses feature a pulse width of 150 fs and a focused spot size of 1.1 μm, full-width-at-half-maximum, repeated at a repetition rate of 1 kHz.

The upper arm of the MZM was excited in every scenario. RF SETs from the upper RF line and optical SETs from the output power of the MZM were recorded for several bias points. The biasing effect of the phase shifter on the SETs is decoupled by having the bias of the excited arm fixed, and the bias of the non-excited arm swept. In a second experiment, the bias of the excited arm was swept.

III. Measurement Results

Fig. 3 shows transient signals recorded from the electrical and optical domains of the device. The term "RF transient" refers to the SETs detected from metal contacts of the excited phase shifter, which can potentially reach an output stage of the MZM driver. "Optical transient" refers to a phenomenon known as the optical single-event transient (OSET), as defined by Tzintzarov *et al.* [7]. Optical perturbations in the excited phase shifter affect the power output of the MZM and are detected with a wide-band photoreceiver.

A. RF Single-Event Transients

RF SETs have been recorded for numerous DC bias voltages in order to sample the full range of bias voltages needed to reach a V_π phase shift in these Si MZMs. Since the DUT has a V_π of 9.8 V, DC biases from 0 to -12 V span a wide range of MZM transfer functions. Considering the MZM in the electrical domain, one can simplify the structure to a *pin* diode. SETs in *pin* diodes have been extensively studied in the literature [8].

In the first experiment, the DC bias voltage on the upper arm was swept from 0 to -12 V, while transients were recorded at each step. Meanwhile, the bias on the lower arm is kept constant. Fig. 4 shows the RF transient peak and collected charge of the excited arm while its DC bias voltage is swept.

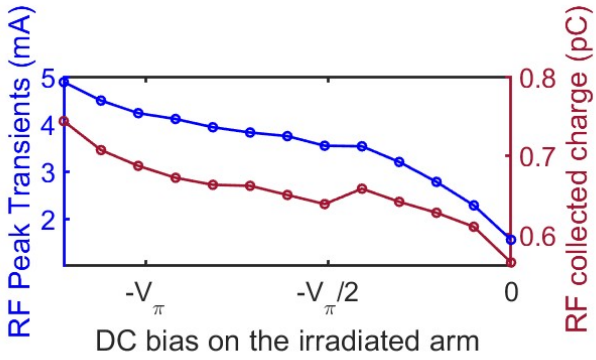

Fig. 4. RF SET's peak and collected charge of the excited MZM when the bias of the excited arm is swept.

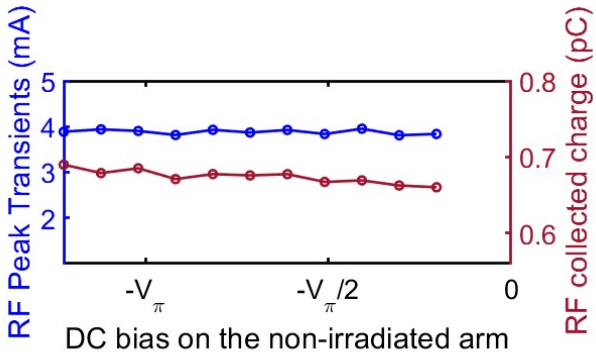

Fig. 5. RF SET's peak and collected charge of the excited MZM when the bias of the non-excited arm is swept. The resulting plots show that biases on each arm of the MZM are isolated.

As expected, the transient peak and collected charge from the excited arm increased with an increasing reverse bias of the upper p-n junction [8].

Afterward, the DC bias voltage on the lower arm is swept from 0 to -12 V, while the bias on the upper arm, which is under the pump laser, was held constant. As shown in Fig. 5, the excited phase shifter's peak transient and collected charge are constant. Changing the bias on one arm does not affect the bias on the other, confirming that biases on two arms of the MZM are electrically isolated.

B. Optical Single-Event Transients

The MZM's sinusoidal output power transfer curve as a function of DC bias is shown in Fig. 6. Four operating points along the transfer function are labeled. To better capture all four points, MZM is biased in a way that the initial phase difference of two arms is set at π. Quadrature-bias points are at DC phase shifts of $-\pi/2$ and $-3\pi/2$, where the output power is half maximum. The Null-bias point is where the DC phase shift is 0, and the output power is 0. The Peak-bias point sits at the DC phase shift of $-\pi$, where the output power is maximum. The manner in which the MZM's output power responds to OSETs is essential at these four points, depending on the chosen modulation scheme [12].

To decouple the effect of DC bias levels on the OSETs, two sets of OSETs versus DC phase shifts have been collected.

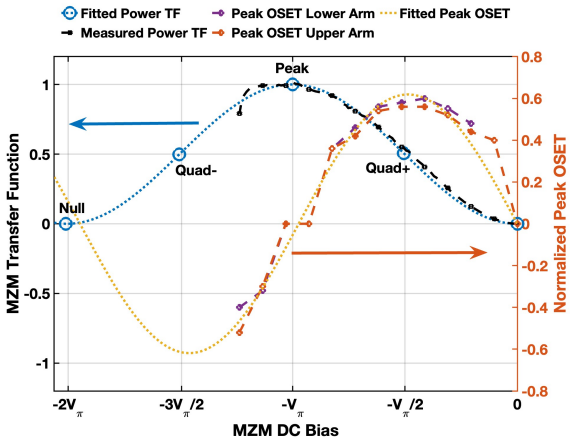

Fig. 6. MZM's measured and fitted transfer function (5) vs. DC bias (DC phase shift) are plotted on the left-hand side. Measured and fitted normalized peak optical transients are shown on the right-hand side. Violet ■ and Orange ■ lines show the peak OSET results of biasing each different arm of the MZM.

Sweeping DC bias on the MZM's separate arms gives us twice the SET data for each operating point, with different DC bias levels in two experiments. Periodic measurements have been performed for each step, and the maximum optical peak transient is reported, in order to account for the worst-case scenario.

The right-hand side of Fig. 6 shows the maximum peak OSETs normalized to the maximum detected power of the MZM, versus various operating points. The fitted curve for peak OSETs shows a sinusoidal profile with a half-period close to V_π. OSETs from two experiments on two arms of the MZM with different DC bias levels exhibit the same trend. It is worth noting that recorded peak OSETs have positive values for the right half of the transfer function, including the Quad+ biasing point. Conversely, negative peak transients are recorded for the other half, including the Quad- biasing point.

Maximum OSET peaks occur at quadrature biasing points, showing more than 50% change in signal level, which is clearly significant. In modulation schemes such as on-off keying (OOK), where MZM is biased at quadrature points, OSETs are thus of major concern.

IV. Analysis and Simulations

To investigate more deeply the physical phenomena behind the effects of OSETs on Si MZMs, we trace the question back to the fundamental theory of electro-optic operation, named by Soref *et al.* [13] as the "plasma dispersion effect" or "free-carrier dispersion" (FCD). Plasma dispersion is the effect that facilitates Si photonics electro-modulation and can be simplified as the perturbation in crystalline silicon's index of refraction by charged carriers in the medium. More recent updated equations describing FCD for 1310-nm light are as follows [14]:

$$\Delta n = -2.98 \times 10^{-22} \Delta N^{1.016} - 1.25 \times 10^{-18} \Delta P^{0.835} \quad (1)$$

$$\Delta \alpha = +3.48 \times 10^{-22} \Delta N^{1.229} + 1.02 \times 10^{-19} \Delta P^{1.089} \quad (2)$$

Where ΔP and ΔN are the free-hole and free-electron concentrations, respectively. in the context of the present paper, $\Delta\alpha$ refers to transient free carrier absorption (TFCA) [15] and Δn refers to a transient change in refractive index.

The model suggests that excess electron-hole pairs (EHPs) induced by laser or heavy ions change the medium's optical properties [7].

Understanding the number of EHPs induced in Si MZM is a significant step toward analyzing OSET effects on the device. Laser-induced techniques for SET testing using TPA have proven to offer numerous advantages in this context [16]. Free carriers generated in Si by TPA have been modeled and are frequently employed for SET testing and simulation [17].

Light traveling through the arm of the MZM, a pin phase shifter, encounters a dense cloud of EHPs generated by the pulsed laser. The additional number of free carriers in the medium affects the optical characteristics of the Si phase shifter. Considering (1) and (2), perturbations in electro-refraction and electro-absorption can be obtained. The EHPs induced in the phase shifter are collected by the electrical field inside the junction and form an electrical transient in the metal contact of the MZM.

The changes in the refractive index of the phase shifter result in a transient phase change as follows:

$$\Delta\Phi[\pi.cm^{-1}] = \Delta\beta_{transient} L = \frac{0.02 * \Delta n_{eff}}{\lambda} \quad (3)$$

Where λ is the frequency of the probe laser, Δn_{eff} and $\Delta\beta_{transient}$ refer to change in the refractive index and propagation constant, respectively, for induced EHPs using (1).

To calculate how the phase shifter's OSET phase and absorption changes result in the MZM's output power transients, the split/combination physics of the MZM was examined. Considering that the input intensity is I_i and the MZM structure is balanced with an optical length of L, the intensity at the output is thus:

$$I_o = \frac{I_i}{4} \left| e^{-j\beta_1 L - \frac{\alpha_1}{2} L} + e^{-j\beta_2 L - \frac{\alpha_2}{2} L} \right|^2 \quad (4)$$

where the propagation of light in each arm is described by $\beta_1 = \frac{2\pi n_1}{\lambda}$ and $\beta_2 = \frac{2\pi n_2}{\lambda}$. For simplicity, the initial phase shifters' losses (α_1,α_2) are considered negligible, and the propagation constant of the non-excited arm (β_2) is considered constant. In this case, equation (4) simplifies to:

$$I_o = \frac{I_i}{2}(1 + \cos(\Delta\beta L)) \quad (5)$$

Where $\Delta\beta = \beta_1 - \beta_2$. Considering $I_{o-max} = I_i$, the normalized peak OSET in MZM output power can thus be simplified to:

$$\begin{aligned} OSET_{MZM} &= \frac{I_{transient} - I_{initial}}{I_{o-max}} \\ &= \frac{e^{-\Delta\alpha L}\cos(\Delta\beta L + \Delta\Phi L) - \cos(\Delta\beta L)}{2} \end{aligned} \quad (6)$$

$I_{transient}$ refers to the optical output power of the MZM when the maximum number of EHPs are induced in the Si DUT. $I_{initial}$ refers to initial MZM output power in (5).

Equation (6) suggests that under the circumstances where transient-FCA dominates ($\Delta\alpha$), peak OSETs will be measured at both null-bias and peak-bias points, where $\Delta\beta L = 0$ or

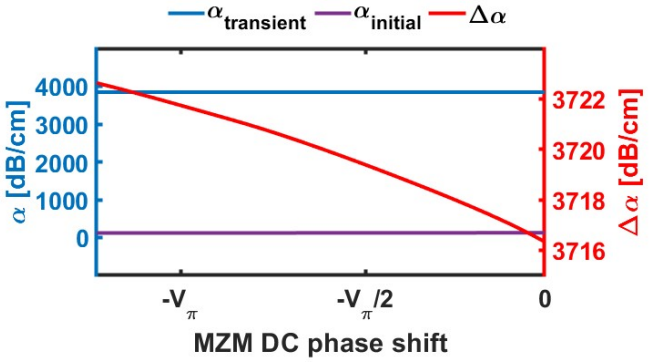

Fig. 7. Simulated absorption coefficients of the initial Si phase shifter and transient state. $\Delta\alpha = \alpha_{transient} - \alpha_{initial}$, added transient-FCA coefficient, is plotted on the right.

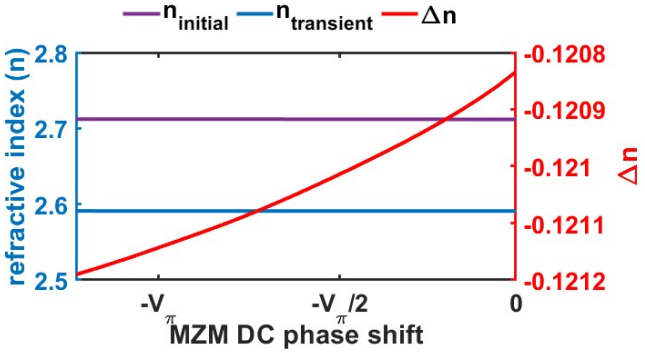

Fig. 8. Simulated refractive index of the initial Si phase shifter and transient state. $\Delta n = n_{transient} - n_{initial}$, the SET-induced change in refractive index, is plotted on the right. The transient phase change can be calculated using (3) and the above numbers.

$\pm\pi$. On the other hand, in circumstances where the transient phase change (Δn) dominates, peak OSETs will be seen at quadrature-bias points, where $\Delta\beta L = \pm\frac{\pi}{2}$.

Here, we propose a simulation methodology to validate the accuracy of the proposed analysis. Sentaurus TCAD was used to investigate how the pump laser causes changes in the free carrier density within the phase shifter. A doped Si pin phase shifter was simulated in the Sentaurus TCAD, using the same geometry as the DUT used in the experiment. The charge deposition profile of the pump laser was calculated using [18] and incorporated into the Sentaurus TCAD through their physical model interface.

The resultant induced carrier density was extracted and then imported to Lumerical CHARGE solutions to connect Sentaurus TCAD to the Lumerical finite-difference time-domain (FDTD) solver. Lumerical FDTD solver has the capability to simulate an electromagnetic wave propagating through any given charge density profile. The probe laser beam has been modeled as a Gaussian distribution, with 1.1 μm FWHM and a peak EHP density of 10^{20} cm^{-3}, as calculated with the Sentaurus TCAD distribution model. The charge profile was not calibrated to measurements and is only a means to better understand the trends.

The results from Lumerical FDTD are shown in Fig. 7 and Fig. 8. Considering the pump laser has a Gaussian distribution with 1.1 μm FWHM, transient FCA and transient phase change in the excited phase shifter can be obtained. Simulations show approximately 0.4 dB of transient loss and 0.2 π transient phase change. Using (6) validates the earlier hypothesis that in these ranges of laser-pulse energies, the transient phase change is dominant over transient-FCA. This, in turn, proves why peak OSETs occur at quadrature-bias points.

Although laser-pulse energies used in this paper were intentionally high in order o detect a measurable OSET, more recent studies have demonstrated that heavier ions in the space environment, such as krypton, can potentially generate EHP densities higher than $10^{20}cm^{-3}$ [19]. It's also worth mentioning that more than 50% signal interruption at the quadrature-bias point, the zero-crossing point for many modulation schemes, can deteriorate bit errors significantly. The final paper will investigate MZM's modulation efficiency and its bit-error degradation due to OSETs for various pulse energies, as well as possible mitigation approaches.

V. Summary

The first optical SET data on Si Mach-Zehnder Modulators (MZM) using laser pulses is presented. A theoretical model and a simulation methodology have been offered to calculate OSET effects on Si phase shifters and modulators.

The optical transients observed in the output power of the Si MZM are attributed to two mechanisms. Induced EHPs by laser pulses form a dense cloud of free carriers in the medium, thereby generating TFCA together with transient phase change. These two effects, operating in parallel, change the properties of the light propagating through MZM phase shifters.

Simulations validate that in the range of pulse energies used in the present paper, the transient phase change is dominant over transient FCA. This results in larger optical transients at quadrature-bias points, where the slope of the MZM transfer function is maximal. Especially for modulation schemes that depend on amplitude modulation and zero-crossing at the quadrature-bias point, OSETs can pose significant concerns.

References

[1] Hemmati, *Deep Space Optical Communications*. Wiley, 2006.
[2] "Dsoc," https://www.nasa.gov/missionpages/tdm/dsoc.
[3] Tzintzarov *et al.*, *MDPI Photonics*, vol. 8, no. 4:131, Apr. 2021.
[4] Krainak *et al.*, *SPIE*, vol. 10899, pp. 75–94, Mar. 2019.
[5] Johnston *et al.*, *IEEE TDMR*, vol. 10, no. 4, pp. 449–459, Dec. 2006.
[6] Lalović *et al.*, *IEEE TNS*, vol. 69, no. 7, pp. 1521–1526, Jul. 2022.
[7] Tzintzarov *et al.*, *IEEE TNS*, vol. 68, no. 5, pp. 785–792, Jan. 2021.
[8] Ryder *et al.*, *IEEE TNS*, vol. 68, no. 5, pp. 801–806, May 2021.
[9] Tzintzarov *et al.*, *IEEE TNS*, vol. 69, no. 3, pp. 527–533, Jan. 2022.
[10] Liao *et al.*, *Opt. Express*, vol. 13, no. 8, pp. 3129–3135, Apr. 2005.
[11] Rakowski *et al.*, in *2022 OFC*. doi: 10.1364/OFC.2020.T3H.3
[12] Devgan *et al.*, *Opt. Express*, vol. 17, no. 11, pp. 9028–9039, Dec. 2009.
[13] Soref *et al.*, *IEEE JQE*, vol. 23, no. 1, pp. 123–129, Jan. 1987.
[14] Nedeljkovic *et al.*, *IEEE Photonics*, vol. 3, no. 6, pp. 1171–1180, Dec. 2011.
[15] Goley *et al.*, *IEEE TNS*, vol. 69, no. 3, pp. 518–526, Mar. 2022.
[16] Schwank *et al.*, *IEEE TNS*, vol. 57, no. 4, pp. 1827–1834, 2010.
[17] McMorrow *et al.*, *IEEE TNS*, vol. 49, no. 6, pp. 3002–3008, Dec. 2002.
[18] Hales *et al.*, *IEEE TNS*, vol. 64, no. 3, pp. 1006–1013, Mar. 2017.
[19] Raine *et al.*, *IEEE TNS*, vol. 58, no. 3, pp. 840–847, Jun. 2011.